CHAPTER 4. MATERIALS AND EXPERIMENTAL PROCEDURE

4.1 Material: Polyamide 12

The materials under study were processed using two different techniques, injection molding (*IM*) and selective laser sintering (*SLS*). Specimens made by *IM* were manufactured by *Aries Industrias del Plástico, S.A.*, located in Spain. The raw material employed was the commercial PA-12 *Evonik Vestamid* supplied in the form of pellets, and the parameters during the manufacturing process are included in *Table 4.1*.

The *SLS* fabrication was carried out by *Prodintec*, in Spain, employing an *EOS Formiga P-100* LS machine which uses a CO_2 laser configured with the optimum process parameters, which are contained in *Table 4.2*. The commercial PA-12 powder suitable for *SLS* was neat PA-12 EOS PA2200.

The technical information of the raw materials was supplied by the manufacturers *Evonik* and *EOS*. *Table 4.3* contains the most remarkable properties of *Evonik VESTAMID* and *EOS PA* 2200 reflected in the manufacturers datasheets [135], [136].

Regarding *EOS PA 2200*, the particle size distribution ranged from 40 to 90 µm, being centred on 50 – 60 µm.

Different specimen configurations were manufactured. In the case of *SLS*, due to the anisotropic nature of the process, two batches of specimens were fabricated for each configuration. In the one named 0°, the layered structure

Table 4.1. Manufacturing parameters of IM PA-12 samples.

Mould temperature	Filling time	Holding time	Injection Speed	Injection pressure	Mold clamping force
60 °C	2.1 s	6.5 s	6-8 mm/s	10 MPa	1500 kN

Table 4.2. Manufacturing parameters of SLS PA-12 samples.

Particle diameter	Powder bed temperature	Frame temperature	Layer thickness	Laser power
40 – 90 µm	171.5 °C	135.5 °C	0.2 mm	25 W

was disposed in such a way that the force was applied parallel to the layer planes; meanwhile in the batch named 90°, the layers were perpendicular to the applied force (*Figure 4-1)*.

Table 4.3. Evonik and EOS PA 2200 properties*[135], [136]*.

	Evonik VESTAMID	EOS PA 2200
Bulk density	-	> 0.43 g/cm^3
Processed density	1.015 ± 0.005 g/cm^3	0.93 ± 0.25 g/cm^3
Melting temperature	178°C	184 °C
Crystallization temperature	-	138 °C
Softening temperature 50 °C/h 50N	140°C	163 °C
Tensile strength	46 ± 1 MPa	45 ± 3 MPa
Young's modulus	1475 ± 120 MPa	1700 ± 150 MPa
Elongation at break	> 50 %	20 ± 5 %
Flexural modulus	-	1240 ± 130 MPa
Charpy-Impact strength	-	53 ± 3.8 kJ/m^2

Figure 4-1. Dumbbell and compact tension (CT) specimens oriented at 0 ° and at 90°. Sintered layers on each orientation are outlined.

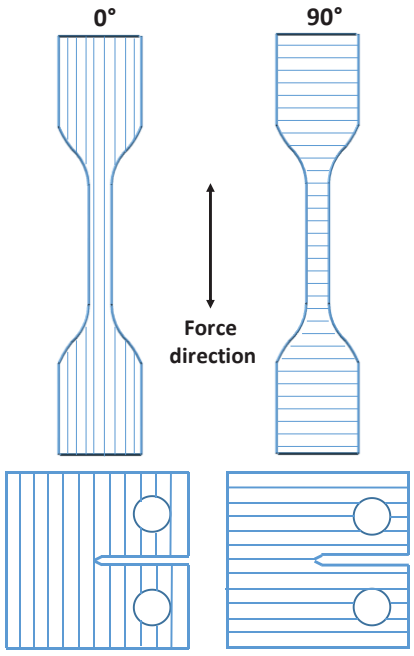

4.2 Physical characterization

4.2.1 Density measurement

Despite the theoretical densities provided by the manufacturers, the experimental ones were measured in the specimens produced. The density of the pieces was determined experimentally measuring 5 specimens of each geometry in a precision balance *Mettler Toledo AX205 DeltaRange®,* which has a resolution of ± 0.00001 g. Following the Archimedes principle, each specimen was introduced in a beaker with a known immersion medium and measuring the amount of displace fluid. The density of the sample, ρ, is given by the following expression:

$$\rho = \frac{W_{air}}{W_{air} - W_{im}}\left(\rho_0 - \rho_L\right) + \rho_L \tag{4-1}$$

where W_{air} is the weight of sample in air, W_{im} is the weight of sample in the immersion medium, ρ_0 is the density of the immersion medium and ρ_L the density of air (0.0012 g/cm$_3$). Due to the nearness of the expected PA-12 density to that of distilled water, commonly used as immersion medium, which is ρ_0= 0.99782 g/cm^3, acetone was also employed as immersion medium in this case, with ρ_0= 0.787 g/cm^3. The closed porosity of each batch was calculated in reference to the theoretical bulk density value of 1.02 g/cm^3 of the PA-12 [137]. Five replicas were measured for each material and condition.

4.2.2 Surface Roughness tests

Surface roughness was measured using a roughness tester *Mitutoyo SJ-301* equipped with a detector whose tip had a radius of 60 µm and a tip angle of 60°. A total number of 62 tests were carried out in the dumbbell geometry of each material longitudinally and transversely. The profile roughness parameters obtained were the maximum peak to valley height of the profile, R_z, and the arithmetical mean value of the tested profile along a length l_r, R_a, given by:

$$R_a = \frac{1}{l_r}\int_0^{lr} \left|z(x)\right| dx \tag{4-2}$$

4.3 Microstructural characterisation

The microstructural characterisation aims to analyse the crystalline phase, focusing on its morphology and its size. For *SLS* PA-12, films between 3 and 15 µm in thickness were sectioned from the centre of the bulk using a rotary microtome *Leica RM2255* [138]–[140]. The extractions were performed parallel and perpendicular to the build direction. Although the anisotropy is not

a key microstructural factor in *IM* specimens, an initial optical inspection revealed some differences between the core and the skin of the material. The same procedure as in *SLS* material was followed for *IM*, that is, the films were extracted from either the core or the skin of the bulk specimen. These films were placed on microscope glass slides and analysed in an optical microscope *Motic BA310 Met-T* equipped with a 5 megapixels *ZEISS Axiocam 105* camera. For their inspection, transmitted polarized light and dark field modes were applied [141]. A total number of 90 micrographs were explored, 30 of *SLS* at 0° orientation, 40 of *SLS* 90° at orientation and 20 of *IM*. The images of the *SLS* specimens were taken using a 50x objective with a 10x eyepiece lens, whereas for the examination of the *IM* films, a x100 objective lens immersed in a transparent oil with a 1.482 refraction index to attain a total magnification of x1482 was needed for the visualization of the characteristic microstructural features.

A total number of 157 spherulites were measured manually using an image analysis software.

4.4 Thermal characterisation

The purpose of the thermal characterisation was to determine the thermal properties and the crystallisation characteristics of *SLS* PA-12 and *IM* PA-12.

Firstly, a Differential Scanning Calorimetry (*DSC*) was performed with a *DSC Mettler 822e* equipment. *DSC* tests consisted in using specimens with 12.0 ± 0.5 mg in weight which were subjected to a heating ramp at a rate of 10 °C/min from 25 °C to 250 °C, followed by a cooling ramp at a rate of 10 °C/min from 250 °C to 25 °C. This heating/cooling processes were performed twice in a row. The crystallisation temperature, T_c, and the enthalpy, ΔH_c, were collected from the cooling cycle, meanwhile the melting temperature T_m and the enthalpy, ΔH_m, and, when detectable, the glass transition temperature, T_g, were extracted from the second heating cycle.

Regarding the calculation of the crystallinity degrees, it was distinguished between the melting crystallinity degree, χ_m, and the crystallinity degree from the crystallisation peak, χ_c. In case of the former, the heat of fusion, $\triangle H_m$, was obtained by integrating the heat flow under the melting peak from the second heating cycle; and for the latter and in a similar way, the crystallization heat, $\triangle H_c$, was also calculated by integrating under the crystallisation peak from the cooling cycle. Finally, the crystallinity degrees were computed using the following equations:

$$\chi_m = \frac{\Delta H_m}{\Delta H_0} \quad ; \quad \chi c = \frac{\Delta H_c}{\Delta H_0} \tag{4-3}$$

using an enthalpy of fusion, △Ho = 209 J/g, which is the enthalpy of fusion of perfect PA-12 crystals [142]. The crystallinity degrees were calculated as the average value from χ_m and χ_c.

Additionally, Dynamic Mechanical Analysis (DMA) was carried out using a *TA Instruments DMA Q800* analyser with a single cantilever configuration according to ASTM D5023 Standard [143]. Specimens with 17×12×3 mm^3 in size were heated from - 100 °C to 150 °C at 1 Hz of frequency and at a heating rate of 3 °C/min. The glass transition temperatures were computed as the maximum values of the loss factor (*tanδ*) curves.

4.5 Mechanical characterisation

Tensile tests were carried out according to ASTM D638 Standard [144] to determine mechanical properties such as tensile strength, Young's modulus, Poisson's ratio and elongation at break. These tests were done using dumbell type IV specimens with the dimensions shown in *Figure 4-2*.

Tests were carried out at -50 °C, 23 °C and 50 °C at 0° and 90° orientations in *SLS* specimens and at 23 °C in *IM* samples. A universal electromechanical testing machine *MTS Alliance RF/100* equipped with a load cell of ± 5 kN was

Figure 4-2. Tensile dumbbell specimens with dimensions according to ASTM D638 [144].

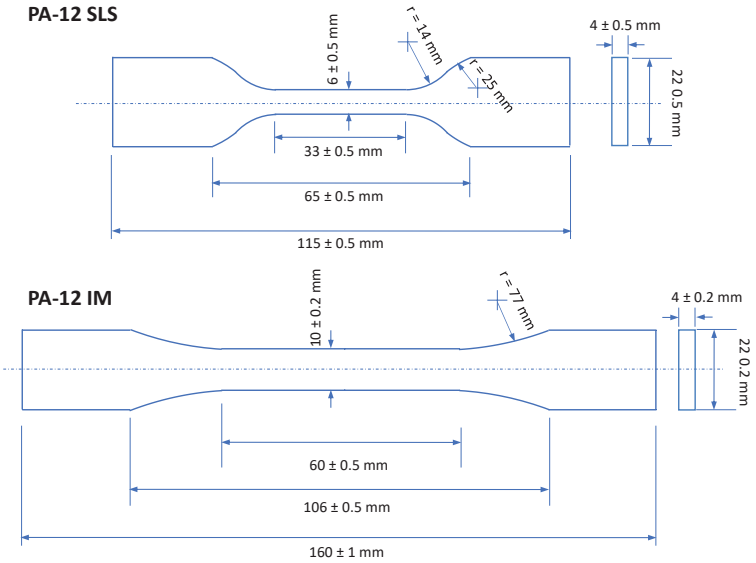

employed. The crosshead speed was 5 mm/min and a contact extensometer *MTS 634.12F-54* (*Figure 4-3*) was used for measuring the axial deformation. A total number of three valid repetitions were performed for each condition. For the tests at -50 °C and 50 °C, the load train, formed by the hinges, grips and the specimen with the extensometer, were placed inside an environmental chamber *MTS 651.06E-03* (*Figure 4-3*). Cooling and heating processes were performed maintaining a constant load of 100 N on the specimen for balancing the thermal contractions. When the required temperature was reached, conditioning was held for a minimum of 30 minutes to reach a stationary state before starting the test.

In addition, 2-Dimensional video correlation was used at all temperatures for obtaining the 2D displacement field and, in particular, the longitudinal and the transverse deformation using a VIC 2D videoextensometer. This equipment consisted of a *PointGrey Grasshopper3* 5 Megapixel camera connected to a computer with the software *Correlated Solutions VIC 2D*. Because videoextensometry needs reference points to follow their movement during the test, the surface of the white specimens were sprayed with black paint to attain a random, matte pattern of speckles, providing a large quantity of points to be analysed, as shown in *Figure 4-4*.

Moreover, to obtain the best possible contrast in the images, LED lightening systems were employed to avoid any type of reflection of the specimen surface. The camera must be focused on the specimen perpendicularly to its lateral surface. The tensile test assembly at room temperature is shown in *Figure 4-5*.

Figure 4-3. MTS Alliance RF/100 with environmental chamber MTS 651.06E-03 and load train installed for tensile tests at -50 °C and 50 °C.

Figure 4-4. Tensile specimen painted with a random dot pattern.

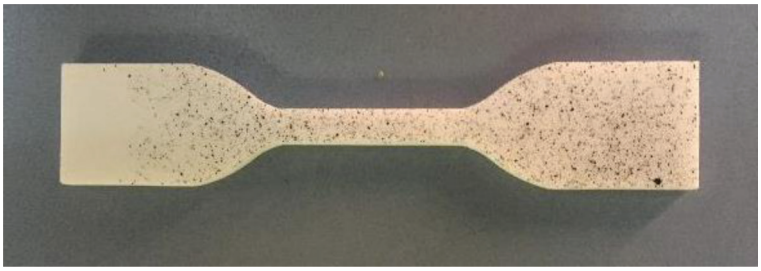

Figure 4-5. MTS Alliance RF/100 equipped for tensile tests at room temperature, with contact extensometer MTS 634.12F-54 and VIC 2D videoextensometer.

4.6 Fracture and fatigue tests

4.6.1 Crack sharpening

Compact Tension (CT) configuration with the dimensions shown in *Figure 4-6* was used for fracture and fatigue tests. The only difference between fracture and fatigue specimens was the initial notch length, which in the fatigue specimens was the half that in fracture ones in order to fulfil ASTM D5045 standard [145] in fracture and ASTM E647 standard [146] in fatigue characterisations.

The sharp crack in the fracture CT specimens was generated by tapping a razor blade with a thickness of 0.3 mm, previously frozen at liquid nitrogen temperature (-196 °C), on the root of the machined notch till attaining an initial natural crack length to width ratio, a_0/W, of 0.5. This ratio ensures a sharp crack length enough to avoid the influence of the manufactured notch on the results [43], [145].

Figure 4-6. Compact Tension (CT) specimen dimensions used in fracture tests according to ASTM D5045 standard [145] and in fatigue tests according to ASTM E647[146].

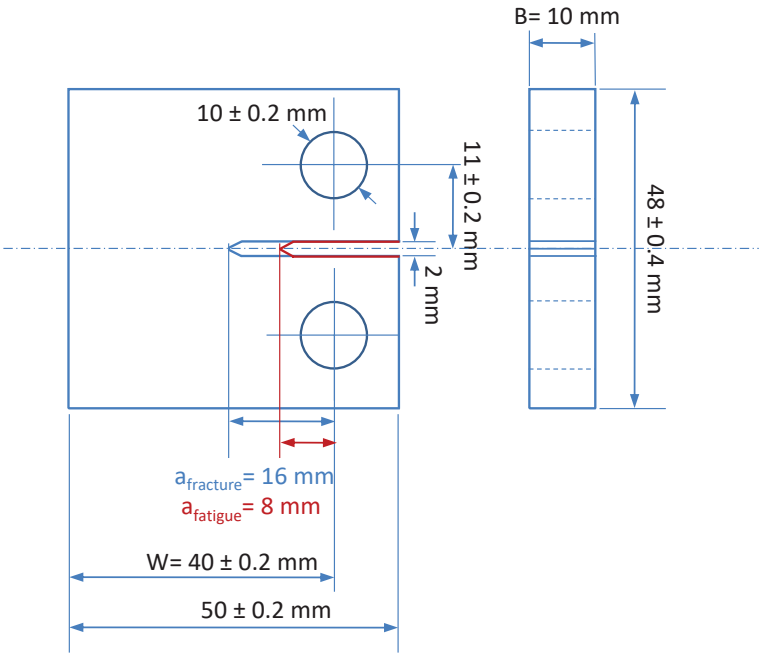

In the fatigue CT specimens, the sharp crack was introduced by tapping in a similar way as in the fracture samples but, in this case the sharp crack lengths should be only larger than the notch height, of 2 mm, to avoid the notch effects [43], [146].

Small cracks were introduced in dumbbell specimens with lengths of 0.2 mm, 0.3 mm, 0.5 mm, 1 mm, 2 mm, 2.5 mm and 3 mm by pressing a microtome razor blade with a tip diameter of 5.3 µm (*Figure 4-7*). This tip diameter ensures a notch radius smaller than 10 µm, which is the estimated limit for considering the crack as a natural crack [147], [148]. These specimens were used for static and fatigue characterisations in the *PSC* regime (*section 2.4)*

After notch sharpening or small crack introduction, the crack front was inspected either visually or by optical means to guarantee no damage in form of microcracks or whitening. In case of presence of damage, the samples were discarded.

Figure 4-7. SEM image of the razor blade tip of the microtome with the diameter measurement [148].

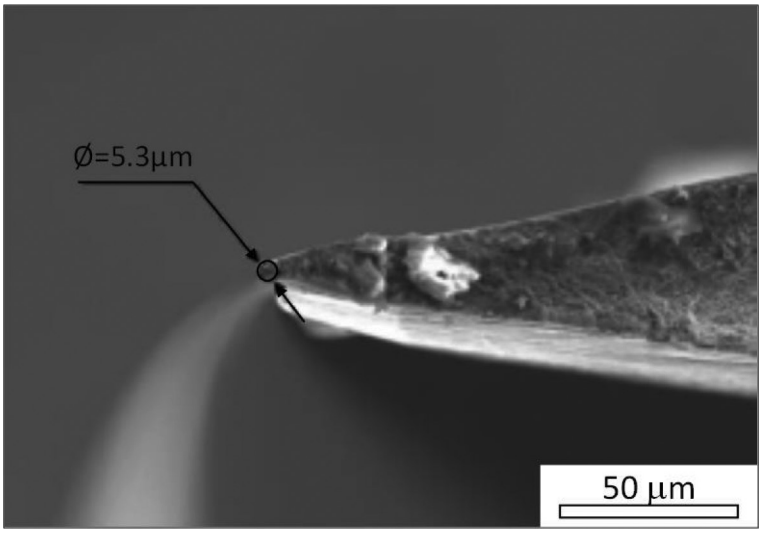

4.6.2 Fracture tests

Tests were carried out in a universal servohydraulic testing machine *MTS 810 Materials Testing*, equipped with a load cell of ± 5 kN. The crosshead speed was 5 mm/min. A Crack Opening Displacement transductor (*COD*) *MTS 632.02F-20* with a displacement range of + 3.9 mm/ -2 mm was also employed. The tests were performed in *SLS* specimens at 0° and 90° orientations, and in *IM* samples. To study the evolution of the fracture properties with the temperature, tests were undertaken at three different temperatures, -50 °C, 23 °C and 50 °C, completing three repetitions of each condition. For the -50 °C and 50 °C tests, an environmental chamber *MTS 651.06E-03* was used, installing the load train, formed by the hinges, grips and the specimen with the *COD* transductor, inside it (*Figure 4-8*).

Similar procedure to that of the tensile tests was performed, maintaining a constant load of 50 N on the specimen during cooling and heating processes until the load frame finished of balancing the thermal contractions and, consequently, reaching a stationary state. When the required temperature was reached, conditioning was held 25 min more before starting the test to guarantee the thermal equilibrium.

Figure 4-8. Load train assembly inside environmental chamber MTS 651.06E-03 for tests at -50 °C and 50 °C.

Attending to the mechanical behaviour of each material and test condition, the results were analysed applying the Linear Elastic Fracture Mechanics (*LEFM*) or the Non-Linear Fracture Mechanics (*NLFM*) approach as appropriate. The ISO 13586 Standard was followed to determine the crack opening mode (mode I) fracture toughness in terms of the stress intensity factor, K_{IC}, and the energy release rate, G_{IC}, under *LEFM* approach [149].

From the load (*P*)-crack mouth opening displacement (*v*) record, the maximum load, P_{max}, and a conditional load, P_Q, are calculated. P_Q is used to determine a conditional stress intensity factor, K_Q, and a conditional energy release rate, G_Q.

Firstly, $P_{5\%}$ is computed as the intersection of the *P-v* record with a line having a 5% smaller stiffness than the initial one, *S*. If the maximum of the curve falls within the best straight line to determine *S* and the line with a 5% lower stiffness, then Pmax corresponds with the load at crack growth initiation, P_Q. If P_{max} falls outside these two lines, then P_Q is $P_{5\%}$. If $P_{max}/P_Q < 1.1$ then P_Q is used for K_Q calculation, otherwise, the test is invalid. With this limitation, the critical stress intensity factor K_Q is obtained:

$$K_Q = f(\alpha)\frac{P_Q}{B\sqrt{W}} \tag{4-4}$$

with *B* the specimen thickness, *W* the width and *f(α)* the geometry calibration factor depending on the crack length *a* given by:

$$f(\alpha) = \frac{(2+\alpha)}{(1-\alpha)^{3/2}}(0.886 + 4.64\alpha - 13.32\alpha^2 + 14.72\alpha^3 - 5.6\alpha^4) \tag{4-5}$$

being $\alpha = a/W$.

In addition to the previous condition, the standard establishes that to guarantee the plane-strain state, it must be fulfilled:

$$B, W-a, a \geq 2.5\frac{K_Q^2}{\sigma_y^2} \tag{4-4}$$

with σ_y the yield stress of the material for the temperature and loading rate of the test and K_Q is K_{IC} in this case. The energy release rate, G_Q is G_{IC} and in principle it can be obtained from the following equation:

$$G_{IC} = \frac{(1-v^2)K_{IC}{}^2}{E} \tag{4-7}$$

E is the Young's modulus and *v* the Poisson's ratio obtained at the same time and temperature conditions. Due to the many uncertainties introduced by this procedure, particularly, in the determination of the Young's modulus, G_Q is computed from:

$$G_Q = \frac{U_Q}{BW\varphi(\alpha)} \tag{4-8}$$

where U_Q is the energy obtained from the area under the P-v curve until the point P_Q and ϕ *(a/W)* is the energy calibration factor depending on the crack length given by this expression:

$$\varphi(a/W) = \frac{A'(1-\alpha)}{H+2A'} \tag{4-9}$$

with

$$A' = 1.9118 + 19.118\alpha - 2.5122\alpha^2 - 23.226\alpha^3 - 20.54\alpha^4 \tag{4-10}$$

and

$$H = \left(19.118 - 5.0244\alpha - 69.678\alpha^2 + 82.16\alpha^3\right)(1 - \alpha) \tag{4-11}$$

When the behaviour of the material deviates from *LEFM,* the J-integral vs. crack growth resistance (J-R) curves were obtained directly from the force displacement record according to ASTM E1820 standard using the normalization method [150]. The starting point of this procedure is the measurement, by optical means, of the initial crack length, a_o, and the final crack length, a_f, taken from the fracture surface. Then, each force value P_i is normalized up to but without including the maximum value P_{max}, following the expression:

$$P_{Ni} = \frac{P_i}{WB\left[\frac{W - a_{bi}}{W}\right]^{\eta pl}} \tag{4-12}$$

where η_{pl} is the plastic constriction factor, which depends on the specimen geometry and is given by:

$$\eta_{pl} = 2 + \frac{0.522\left(W - a_0\right)}{W} \tag{4-13}$$

and a_{bi} is the crack growth applying the blunting correction:

$$a_{bi} = a_0 + \frac{J_i}{2\sigma_y} \tag{4-14}$$

where

$$J_i = \frac{K_i^2\left(1 - v^2\right)}{E} + J_{pl,i} \tag{4-15}$$

with K_i the stress intensity factor obtained from eq. (*4-4*) and eq. (*4-5*) and $J_{pl,i}$ the plastic component of the J-integral:

$$J_{pl,i} = \frac{\eta_{pl} U_i}{B\left(W - a_0\right)} \tag{4-16}$$

where U_i is the area under the curve until P_i.

The displacement corresponding with each force level P_i, δ_i, is also normalized to use a plastic normalized displacement, δ'_{pli}:

$$\delta'_{pli} = \frac{\delta_{pli}}{W} = \frac{\delta_i - P_i C_i}{W} \tag{4-17}$$

being C_i the specimen elastic load-line compliance using the crack length a_{bi}. The same procedure is employed to obtain the last point, at P_{max}, but using, the measured final crack length, a_f, instead of a_o, the P_{Ni}-δ'_{pli}values are fitted to the normalized function:

$$P_N = \frac{a + b\delta'_{pl} + c\delta'^{\,2}_{pl}}{d + \delta'_{pl}} \tag{4-18}$$

with a, b, c and d the fitting parameters. Once these parameters are determined, a_i values are calculated using an iterative method.

Finally, with the force, the displacement and the crack size estimated at each point, the J integral value for each i point was determined using:

$$J_i = \frac{\eta U_i}{B\left(W - a_i\right)} \tag{4-19}$$

With $\eta = \eta_{pl}$ for the CT configuration and the crack extension, Δa, as:

$$\Delta a = a_i - a_0 \tag{4-20}$$

The resulting J-crack growth resistance curve is fitted to a power law $J = C_J \Delta a^{N_J}$ with $N_J < 1$. The crack initiation resistance, J_{IC}, is calculated as the minimum value between $J_{0.2}$, which defines crack resistance at 0.2 mm of the total crack growth, and J_{BL}, computed as the intersection between the crack growth resistance curve and the blunting line defined as:

$$J_{BL} = 2\sigma_y \Delta a \tag{4-21}$$

The size requirements for plane strain J_{IC} is given by [151]:

$$B, a, W - a > 25\frac{J_{IC}}{\sigma_y} \tag{4-22}$$

The normalized method was applied using the MATLAB® script included in the *Annex A.1*.

4.6.3 Fatigue crack growth tests

The fatigue tests were carried out under the recommendations of the ASTM E647 Standard [146] and ESIS TC4 protocol [152], which aim to obtain the crack propagation threshold value of the control parameter and the fatigue crack propagation curves.

A total number of eight samples of *IM* material and fourteen samples of each *SLS* orientation were tested at room temperature in a servo-hydraulic testing machine *MTS 810 Materials Testing* with a load cell of ± 5 kN and a crack opening displacement (*COD*) extensometer MTS 632.02 F-20 with a displacement range of +3.9 mm/-2 mm (*Figure 4-9*). The tests were carried out at room temperature (23°C), with a frequency of 1 Hz, load ratio R = P_{min}/P_{max} of 0.1 and imposing a sinusoidal load wave. Two test procedures were used according to ASTM E647.

To obtain the crack propagation behaviour until failure, five *IM* specimens and ten *SLS* specimens per orientation were tested in constant-force-amplitude configuration or increasing control parameter mode. On the other hand, to obtain the crack propagation threshold, three *IM* specimens and four *SLS* specimens per orientation were tested under the decreasing control parameter procedure. Beginning with a control parameter value under the critical value obtained from the fracture tests, tests with decreasing load amplitude

Figure 4-9. MTS 810 Materials Testing machine configured for performing fatigue crack growth tests in CT specimens.

were carried out with a step of decrease or normalized variation of the control parameter of -0.05 mm^{-1}. The threshold values were computed for crack growth rate downs to $3 \cdot 10^{-7}$ mm per cycle.

Two methods were used for obtaining the crack growth during the tests. In the first method, the crack growth was calculated by the compliance method from the flexibility of the specimen using expressions determined for metals but also validated for polymers [152]. The expressions that relate the crack length to width ratio, a/W, with the compliance in *CT* specimens are

$$\frac{a}{W} = 1.001 - 4.6695\,U + 18.460\,U^2 + 236.82\,U^3 + 1214.9\,U^4 - 2143.6\,U^5 \tag{4-23}$$

where:

$$U = \frac{1}{\left(\frac{BE\mathrm{v}}{P}\right)^{1/2} + 1} \tag{4-24}$$

To validate the compliance method, an optical method was used. Images were captured during the test at a specific frequency allowing the tracking of the crack length with a millimetre scale stuck to the specimen's surface. Moreover, the calculated final crack length was compared with the measured fatigue crack length on the fracture surface of each specimen.

The fatigue behaviour has been determined as the crack growth rate, *da/dN,* versus the Crack Driving Force, *CDF*, $\Delta\sqrt{G}$ according to *equation (2-2)*.

The crack growth rate at any average crack length $\overline{a} = \frac{a_{i+1} - a_i}{2}$ is obtained

from the crack length versus elapsed cycle with the following expression:

$$\left(\frac{da}{dN}\right)_{\overline{a}} = \frac{a_{i+1} - a_i}{N_{i+1} - N_i} \tag{4-25}$$

The control parameter $\Delta\sqrt{G}$ was obtained from *equation (2-1)* in which the value of *dC/da* is given by:

$$\frac{dC}{da} = \frac{1}{EW}\frac{dg}{d\alpha} \tag{4-26}$$

where *g(α)* is the non-dimensional load line compliance [26] and with dg/dα

for CT specimens computed as:

$$\frac{dg}{d\alpha} = \frac{(1+\alpha)}{(1-\alpha)^2} x \qquad (4\text{-}27)$$

$$\left[\frac{4}{(1-\alpha)}\left(2.163 + 12.219\alpha - 20.065\alpha^2 - 0.9925\alpha^3 - 20.609\alpha^4 - 9.9314\alpha^5\right)\right.$$
$$\left. + (1+\alpha)\left(12.219 - 40.13\alpha - 2.9775\alpha^2 + 82.436\alpha^3 - 49.657\alpha^4\right)\right]$$

4.6.4 Fatigue life tests

Fatigue life tests were performed to obtain S-N curves for *IM* and *SLS* specimens at both orientations, according to ASTM D7791 Standard [153]. The specimens had the same geometry and dimensions as those utilized in tensile tests (*Figure 4-2*). A total number of 89 specimens were tested, of which 20 were used for the determination of *IM* PA-12, 32 for *SLS* PA-12 at 90° orientation and 37 for PA-12 at 0° orientation. Tests were performed at room temperature in a servo-hydraulic testing machine *MTS 810 Materials Testing* with a load cell of ± 5 kN. A contact extensometer *MTS 634.31F-24* with a displacement range of +4 mm/-2 mm was employed to measure the axial strain.

The frequency was 1 Hz, using a sinusoidal load wave form at a constant load amplitude with a load ratio, *R*, of 0.1. Tests were done at 12 different stress levels, that is with the maximum stress of the cycle, σ_{max}, to the tensile

Figure 4-10. MTS 810 Materials Testing set for fatigue life tests.

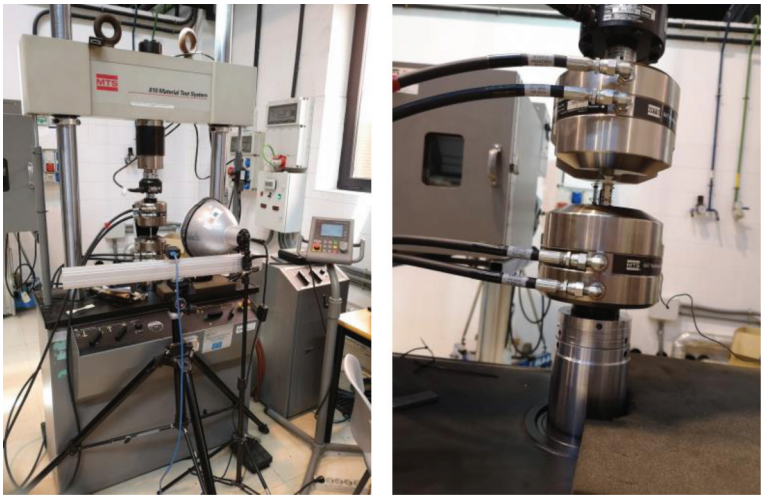

strength ratio between 58.75% and 85%, to guarantee to be within the High Cycle Fatigue regime. At least, two repetitions for each stress level were carried out.

The tests at the lowest levels were finished at 10^6 cycles due to their high timeconsuming aspect, establishing tests which reached this number of cycles without failure as run-outs. Each test was plotted as a single point of the stress range, $\Delta\sigma$, versus N representation, giving as result the Wöhler curve for each material.

The fatigue life curves were fitted to the Basquin equation:

$$\Delta\sigma = B_B N^{mB} \tag{4-28}$$

The estimated value of the fatigue limit, $\Delta\sigma_{fl}$, at 10^6 cycles were determined by the maximum likelihood method, following a test sequence based on the staircase method. In this method, fatigue tests were sequenced at different stress levels with a fixed difference in the applied stress range or initial step of 2.5% of the tensile strength. If a specimen failed before reaching the end of the test, the following test was carried out at a stress level one step lower. Otherwise, the stress level was increased one step in the following test. To obtain a more accurate value, the step was decreased after seven completed tests to 1.25% of the tensile strength. Although the change in the step removed the possibility of using the Staircase method equations developed for metals [154], the maximum likelihood method allowed to obtain an accurate estimation of $\Delta\sigma_{fl}$ [155]–[157]. A total number of 17 for *SLS* PA-12 specimens at 0° orientation, 12 for PA-12 samples at the 90° orientation and 14 for *IM* material were tested to obtain $\Delta\sigma_{fl}$.

The maximum likelihood method was applied assuming that the stress levels of the run-out specimens follow a normal distribution [156], [158]. For a normal distribution with a mean value, μ, and a standard deviation value, s, the likelihood function, L, is given by:

$$L = \prod_{i=1}^{n_T} \left[1 - F\left(\Delta\sigma_i, \mu, s\right)\right]^{r_i} \left[F\left(\Delta\sigma_i, \mu, s\right)\right]^{f_i} \tag{4-29}$$

where r_i are the number of run-outs and f_i are the number of failures at the i^{th} stress level, $\Delta\sigma_i$, n_T is the total number of stress amplitude levels and F is the cumulative probability of failure of the normal distribution.

This function depends on the stress at the i^{th} stress level, $A\sigma_i$ and the parameters of the normal distribution and is calculated with the following expression:

$$F\left(\Delta\sigma_i,\mu,\sigma\right)=\int_{-\infty}^{\Delta\sigma_i}\frac{1}{s\sqrt{2\pi}}\exp\left[-\frac{1}{2}\left(\frac{\mu-x}{s}\right)^2\right]dx \tag{4-30}$$

The maximum of the likelihood function was obtained using the MATLAB® script proposed by Meizoso et al. [155] and included in the *Annex A.2*.

4.6.4.1 Determination of fracture parameters from damage evolution in plain fatigue samples using the Fracture Mechanics methodology

The fracture toughness was calculated from the measurement of the damage observed and measured from the analysis of the morphology of the fracture surfaces resulting of the fatigue life tests in *SLS* PA-12. The extent of the damage was delimited, that is, the limit associated with the area of crack propagation before instability occurred was determined from the optical and Scanning Electron Microscopy (*SEM*) inspections of the fracture surfaces. The crack nucleated at some point at the surface due to the elevated roughness resulting from the manufacturing process.

The geometrical configuration of the fatigue specimens with a crack growth zone resulting from the crack propagation stage before failure could be assimilated to the Single Edge Notch Tension (*SENT)* fracture specimens.

The fracture parameters were determined using the *NLFM* approach and the J-integral at the instant of failure was computed as

$$J=\frac{\eta U}{B(W-a)} \tag{4-31}$$

where *U* is the area under the unloading load-displacement record of the last cycle before failure, a is the length of the subcritical crack growth zone measured directly from the fracture surface and η is a plastic geometric factor that in case of the SENT configuration is defined as [159]:

$$\begin{aligned}\eta=1.067-1.767\left(\frac{a}{W}\right)+7.808\left(\frac{a}{W}\right)^2\\ -18.269\left(\frac{a}{W}\right)^3+15.295\left(\frac{a}{W}\right)^4\\ -3.083\left(\frac{a}{W}\right)^5\end{aligned} \tag{4-32}$$

4.7 Fractography

The fracture surfaces of the tensile, fracture, fatigue crack growth and fatigue life specimens were inspected using scanning electron microscopy. The aim was to determine the micromechanisms of failure dominant at different temperatures, orientations and different manufacturing conditions. The fracture surfaces were gold coated to enhance their conductivity using a sputter coater *EMITECH K550X* with a current of 30 mA for 1 minute. The coated samples were positioned on a conductive specimen holder and examined in a *SEM HITACHI S-3400N*.